

Elastin-like-recombinamers multilayered nanofibrous scaffolds for cardiovascular applications

This content has been downloaded from IOPscience. Please scroll down to see the full text.

2016 Biofabrication 8 045009

(<http://iopscience.iop.org/1758-5090/8/4/045009>)

View [the table of contents for this issue](#), or go to the [journal homepage](#) for more

Download details:

IP Address: 157.88.202.123

This content was downloaded on 10/04/2017 at 15:02

Please note that [terms and conditions apply](#).

You may also be interested in:

[Electrospun scaffolds functionalized with heparin and vascular endothelial growth factor increase the proliferation of endothelial progenitor cells](#)

D I Braghirolli, V E Helfer, P C Chagastelles et al.

[Current approaches to electrospun nanofibers for tissue engineering](#)

Nae Gyune Rim, Choongsoo S Shin and Heungsoo Shin

[The effects of PHBV electrospun fibers with different diameters and orientations on growth behavior of bone-marrow-derived mesenchymal stem cells](#)

Lan-Xin Lü, Yan-Yan Wang, Xi Mao et al.

[Electrospun fiber scaffolds of poly \(glycerol-dodecanedioate\) and its gelatin blended polymers for soft tissue engineering](#)

Xizi Dai, Khadija Kathiria and Yen-Chih Huang

[Hybrid fluorescent curcumin loaded zein electrospun nanofibrous scaffold for biomedical applications](#)

Dhandayuthapani Brahatheeswaran, Anila Mathew, Ravindran Girija Aswathy et al.

[Improved cellular infiltration into nanofibrous electrospun cross-linked gelatin scaffolds](#)

Maciej Skotak, Jorge Ragusa, Daniela Gonzalez et al.

[Functionally graded nanofibrous scaffolds](#)

Vinoy Thomas, Xing Zhang, Shane A Catledge et al.

[Biofabrication of bundles of poly\(lactic acid\)-collagen blends mimicking the fascicles of the human Achille tendon](#)

Alberto Sensini, Chiara Gualandi, Luca Cristofolini et al.

Biofabrication



PAPER

Elastin-like-recombinamers multilayered nanofibrous scaffolds for cardiovascular applications

RECEIVED
7 June 2016

REVISED
10 August 2016

ACCEPTED FOR PUBLICATION
31 August 2016

PUBLISHED
15 November 2016

M Putzu^{1,2}, F Causa^{1,2,3}, V Nele^{1,2,7}, I González de Torre⁴, J C Rodriguez-Cabello^{5,6} and P A Netti^{1,2,3}

¹ Dipartimento di Ingegneria Chimica, dei Materiali e della Produzione Industriale (DICMAPI), University 'Federico II', Piazzale Tecchio 80, 80125 Naples, Italy

² Interdisciplinary Research Centre on Biomaterials (CRIB) University of Naples Federico II Piazzale Tecchio 80, 80125 Napoli, Italy

³ Center for Advanced Biomaterials for Health Care@CRIB Istituto Italiano di Tecnologia, Largo Barsanti e Matteucci 53, 80125 Napoli, Italy

⁴ Technical Proteins NanoBioTechnology S.L., Edificio CTTA, Paseo de Belen, 9A, 47011 Valladolid, Spain

⁵ Bioforge Lab, University of Valladolid, Edificio LUCIA, Paseo de Belen, 19, 47011 Valladolid, Spain

⁶ Networking Research Center on Bioengineering, Biomaterials and Nanomedicine (CIBER-BBN), Valladolid, Spain

⁷ Present address: Material Department Imperial College, Royal School of Mines, Exhibition Road, London SW7 2AZ, UK

E-mail: causa@unina.it

Keywords: electrospinning, multilayered scaffold, cardiovascular device, protein building blocks

Abstract

Coronary angioplasty is the most widely used technique for removing atherosclerotic plaques in blood vessels. The regeneration of the damaged intima layer after this treatment is still one of the major challenges in the field of cardiovascular tissue engineering. Different polymers have been used in scaffold manufacturing in order to improve tissue regeneration. Elastin-mimetic polymers are a new class of molecules that have been synthesized and used to obtain small diameter fibers with specific morphological characteristics. Elastin-like polymers produced by recombinant techniques and called elastin-like recombinamers (ELRs) are particularly promising due to their high degree of functionalization. Generally speaking, ELRs can show more complex molecular designs and a tighter control of their sequence than other chemically synthesized polymers Rodriguez Cabello *et al* (2009 *Polymer* **50** 5159–69, 2011 *Nanomedicine* **6** 111–22). For the fabrication of small diameter fibers, different ELRs were dissolved in 2,2,2-fluoroethanol (TFE). Dynamic light scattering was used to identify the transition temperature and get a deep characterization of the transition behavior of the recombinamers. In this work, we describe the use of electrospinning technique for the manufacturing of an elastic fibrous scaffold; the obtained fibers were characterized and their cytocompatibility was tested *in vitro*. A thorough study of the influence of voltage, flow rate and distance was carried out in order to determine the appropriate parameters to obtain fibrous mats without beads and defects. Moreover, using a rotating mandrel, we fabricated a tubular scaffold in which ELRs containing different cell adhesion sequences (mainly REDV and RGD) were collected. The stability of the scaffold was improved by using genipin as a crosslinking agent. Genipin-ELRs crosslinked scaffolds show a good stability and fiber morphology. Human umbilical vein endothelial cells were used to assess the *in vitro* bioactivity of the cell adhesion domains within the backbone of the ELRs.

Introduction

Atherosclerosis is an inflammatory disease that mainly affects the elastic wall of medium-sized arteries. Inflammation is a component of all forms of plaque (Rosmond *et al* 2007). The thickening of the vessel wall and subsequent occlusion are surgically treated for the reopening through the use of angioplasty surgery.

One of the most important problems after angioplasty surgery is restenosis, an anomalous wound healing process that may occur after some endovascular procedures and that can lead to the appearance of a new narrowing of the blood vessel after 2–6 months of treatment (Suryapranata *et al* 1988, Smith *et al* 1991).

Several vascular grafts have been fabricated through the use of electrospinning using different

A) HIS-TAG $\{[(VPGIG)_2-VPGKG-(VPGIG)_2]_2$ AVTGRGDSPASS $\{[(VPGIG)_2-VPGKG-(VPGIG)_2]_2\}_6$

B) $\{[(VPGIG)_2-VPGKG-(VPGIG)_2]_2$ EEIQIGHIPREDVDYHLYP $\{[(VPGIG)_2-VPGKG-(VPGIG)_2]_2$ (VGVAPG) $\}_3\}_{10}$

Figure 1. Elastin-like-polypeptides primary structures: (A) HRGD6 recombinamer, (B) REDVx10 recombinamer.

types of synthetic polymers, such as PCL or PLGA (Shinoka *et al* 1998). Electrospinning is a simple and versatile top-down approach for fabricating uniform ultrafine fibers in a continuous process. Electrospinning offers several advantages, such as easy control of porosity, fiber size, and morphology among others; an effort has been made to fabricate micro/nanofibers with desired morphologies, such as aligned fibrous array and fibrous patterns (Teo *et al* 2001). The principle of electrospinning operation is based on the application of a high potential difference (kilovolt) between two electrodes. Such electrodes are constituted, respectively, by a capillary metal (cathode) -that contains the molten or dissolved polymer to be processed- and a plate of copper or aluminum (anode)-on which the collection of the fibers takes place (Travis *et al* 2008). Various materials can be electrospun including: biodegradable, non-degradable, and natural materials (Travis *et al* 2008).

An alternative strategy to synthetic and degradable scaffold-based vascular grafts is the manipulation of proteins that constitute the architecture of native ECM. Collagen, elastin and fibrin have been widely used for the manufacturing of biodegradable vascular grafts (Watanabe *et al* 2001, Qijin *et al* 2004). Wise *et al* (2011), synthesized a scaffold by electrospinning human tropoelastin and polycaprolactate. They showed an enhanced endothelial recognition and low thrombogenicity (Wise *et al* 2011). In this context, the development of recombinant genetics and protein engineering enabled the synthesis of bioinspired protein polymers ('recombinamers') that not only mimic structural proteins, but also direct cellular fate by emulating the ECM *in vivo*. Elastin-like polypeptides and in particular their recombinant versions, the elastin-like recombinamers (ELRs), are biomolecules with a great potential as scaffolds for tissue engineering thanks to their unique characteristics (Urry 1992). Thus, in order to combine different features such as elasticity and strength in a single material, some groups produced ELR-based scaffolds using electrospinning. In this work we used two different ELRs to obtain membranes. ELRs had been previously bio-functionalized through the insertion of specific cell recognition sequences, RGD and REDV. We optimized the process parameters in order to obtain fibers without beads and defects. One of the most specific properties of ELRs is their thermal sensitiveness. Below a critical temperature, T_t , whose value is intrinsically dictated mainly by the polarity of the

constituent amino acids and their arrangement along the recombinamer chain (Ribeiro *et al* 2009), the ELRs are water-soluble. Above it, the recombinamer segregates from the solution giving rise to different structures, from simple coacervates to micelles and other nanostructures (Martin *et al* 2012).

However, it has been previously demonstrated that uncrosslinked ELR-based scaffolds are not structurally stable even though they are kept above their T_t s (García-Arevalo *et al* 2012). Due to chain mobility and depending on the ELR composition, the primary structures evolve relatively rapidly to unstructured coacervates or disgregate in the form of different nanoparticles; this is particularly evident for amphiphilic ELRs. For this reason, ELRs have to be cross-linked in order to assess their structural stability. ELR scaffolds and hydrogels have often been crosslinked through the use of various crosslinking agents, such as isocyanates (Paul *et al* 2004), trans-glutaminase (MacHale *et al* 2006) and genipin (Kinikoglu *et al* 2011).

In this work, the stability of electrospun scaffold using genipin as a crosslinking agent was improved. Genipin has been reported to provide material with higher biocompatibility and less toxicity and has been recently used as a crosslinking agent for electrospun gelatin (Panzavolta *et al* 2011). Bioactivity has been already improved by the inclusion of specific cell binding domains within the polymeric structure that allow the recognition and proliferation of cells (García-Arevalo *et al* 2012). Preliminary *in vitro* studies were done in order to assess the efficacy of these bioactive domains.

Methods

Two ELRs containing two different cell adhesion domains, RGD and REDV respectively, were kindly provided by Technical Proteins NanoBiotechnology S. L. (HRGD6, TP20254 and REDVx10, TP20109). Figure 1 shows the polypeptide composition. In both cases the cell binding domains were escorted by VPGIG/VPGKG pentapeptide block repeats that confer elastomeric properties on the resulting recombinamer and crosslinking capabilities through lysine residues (García-Arevalo *et al* 2012). Because of the repeated blocks, polymers possess different molecular weights, which affects their physical and chemical behavior. In particular, RGD molecular weight is 60 kDa while REDV is 84 kDa.

Thanks to the presence of a specific recognition sequence within the recombinamer structure, we built a new nanofibrous scaffold made of two different layers. The inner layer of the scaffold was produced through the electrospinning of the REDV polymer in order to allow the recruitment of the endothelial precursors cells. The REDV tetrapeptide is specifically recognized by the integrin $\alpha_4\beta_1$ present in endothelial cells selectively bound to REDV coated surfaces (Rodriguez Cabello *et al* 2012). The outermost layer was synthesized through the use of the HRGD6 polymer. HRGD6 contains six equally spaced units of the fibronectin derived RGD domain along the recombinamer chain, which represent the primary integrin-binding sequence and the amino acids that maintain the optimal conformation for interacting with integrins. Thus, the RGD sequence will recognize endothelial intima cells.

It has been previously demonstrated that amphiphilic polymers can be dissolved using alogenerated solvents. ELR solutions were prepared using 2,2,2-trifluoroethanol (CAS nr. 75-89-8, purity $\geq 99\%$) purchased from Sigma-Aldrich, Italy. A thorough characterization of the ELR behavior in TFE was carried out by dynamic light scattering (DLS). Measurements were performed between 10 °C and 40 °C using Zeta Sizer Nanosystems (Malvern Instruments, UK). Scaffolds obtained from the ELRs were produced using Nanofiber NF-500 Machine (MECC-LTD, Japan). Fibers with different size and morphology were obtained by varying process parameters.

The fast desegregation or destructure rates of ELR scaffolds in aqueous environments makes it necessary to take additional measures for the stabilization of the fibrous texture, such as the use of a cross-linking agent. For this purpose, we used genipin (CAS nr.6902-77-8 Sigma Aldrich, USA) that allowed the stabilization of the fibrous matrix in aqueous environment.

Preliminary *in vitro* assays were conducted with Human umbilical endothelial vein cells (Invitrogen, LIFE-TECHNOLOGIES, Italy) in order to evaluate the adhesion and proliferation on top of ELR scaffolds, seeding cells on the HRGD6 side. Adhesion of cells on top of such nanofibrous scaffolds was measured using Sytox Green and Phalloidin staining (Sigma-Aldrich, Italy). An MTT cytocompatibility assay (Cell Growth MTT kit Sigma-Aldrich, Italy) assay was used to measure the viability of cells on top of crosslinked genipin scaffolds at 24, 72 h and 1 week.

DLS characterization

Based on the known interactions between trifluoroethanol and polypeptides, we undertook a thorough characterization of the chemical behavior of the polypeptide solutions obtained. DLS experiments were carried out for HRGD6 and REDVx10 solutions

in TFE in order to characterize the behavior of those recombinamers. Measurements were performed between 10 °C and 40 °C, with a stabilization time of 5 min using Zeta Sizer Nanosystem (Malvern Instruments, UK).

HRGD6 and REDVx10 samples were prepared at 150 mg ml⁻¹ in TFE, placed in DLS cuvettes and heated to the final temperature. Twelve runs were performed for each sample in order to determine the particle/aggregate size and to obtain a final average value at constant temperature.

Scaffold fabrication

HRGD6 and REDVx10 were dissolved in 2,2,2-trifluoroethanol (TFE) at a concentration of 15%(w/v). The solutions were maintained under stirring for 1 h at room temperature and then at 4 °C for 24 h, in order to obtain a clear solution. A stable Taylor cone is required for the formation of uniform fibers, so preliminary electrospinning experiments were conducted in order to evaluate the optimal electrospinning conditions. All the electrospinning experiments were conducted with Nanofiber NF-500 Electrospinning Machine (MECC-LTD, Japan). Recombinamer solutions were placed in 6 ml plastic syringes (Norm-Ject Luer Lock) and fitted by a 27 × 15 mm needle. Fibers were collected on a flat aluminum collector using different process parameters for the two recombinamers.

All the flat matrices were left under hood for 24 h, prior to scanning electron microscopy analysis. All surfaces covered with ELR were observed using scanning electron microscopy (FESEM-ULTRAPLUS, Zeiss) in a low vacuum mode. Samples were sputter coated with 10 nm Au (CRESSINGTON 208 HR, High resolution sputter coater) and all the images were collected at 10 kV. SEM images were used to determine fiber diameter and porosity and to check surface homogeneity. Fiber diameters were determined by counting 50 independent fibers using ImageJ software.

Using a 4 mm rotating mandrel collector, we synthesized a tubular scaffold made of an inner layer (REDV layer) and an outer layer (RGD layer). Rotation speed was set at 60 rpm. Electrospinning was carried on for 5 h in order to obtain a composite structure.

Cell culture assay

Human umbilical endothelial vein cells—HUVEC (Invitrogen, LIFE-TECHNOLOGIES, Italy) were cultured in M200 medium (Gibco®, LIFE-TECHNOLOGIES, Italy) and supplemented with low serum supplement kit (LGS kit-Gibco®, LIFE-TECHNOLOGIES, Italy) containing 2% of fetal bovine serum (FBS), basic fibroblast growth factor (3 ng ml⁻¹), human epidermal growth factor (10 ng ml⁻¹), hydrocortisone (1 mg/ml), heparin (10 mg ml⁻¹) and

penicillin/streptomycin ($100 \text{ U ml}^{-1}/100 \mu\text{g ml}^{-1}$), at 37°C in a humidified atmosphere comprising of 5% CO_2 and 95% air.

Prior to cell seeding, all ELR surfaces were sterilized under hood for 1 h using UV light. Medium was changed every 4 h (for 4, 8 and 24 h) during the experiment. Cell passages 5–8 were used in all cells experiments. HUVEC were seeded at a density of 10^4 cells per scaffold on top of dry crosslinked and uncrosslinked ELR surfaces placed on 24-well culture plates on HRGD6 side, and on top of gelatin coated dishes (control samples), after a short trypsin treatment.

After 4, 8 and 24 h loose or unbound cells were removed through trypsin treatment. ELR scaffolds were washed twice with phosphate-buffer saline (PBS). Number of cells adhered during the time of experiment were detached and counted. Cells were fixed with 4% paraformaldehyde (Sigma-Aldrich, Italy). Sytox Green (Invitrogen, LIFE-TECHNOLOGIES, Italy) and phalloidin (dilution 1:200) (Invitrogen, LIFE-TECHNOLOGIES, Italy) were used to visualize cell nuclei and cytoskeleton. Morphology and spreading of stained cells was collected using confocal transmission microscopy (CLSM LEICA, TCS SP5).

For the viability experiments, MTT solution was prepared at 5 mg ml^{-1} with Dulbecco modified eagle medium (DMEM, Gibco®, LIFE-TECHNOLOGIES, Italy) without additional growth factors and FBS. Prior to seeding cells, scaffolds have been cut into $1 \text{ cm} \times 1 \text{ cm}$ disks. HUVEC cells were seeded at a density of 10^4 cells on top of crosslinked scaffolds; at specific time points (24, 72 h and 1 week) scaffolds were washed twice with fresh PBS and treated with the MTT solution. Absorbance at 570 nm has been read, prior to calibration curve.

All the experiments were done in triplicate for all substrates.

Statistical analysis

Data presented are expressed as mean \pm standard deviation of mean (SD). Comparisons between groups were performed by Bonferroni post-hoc test. Statistical significance was set at $p < 0.001$.

Results

An initial investigation focused on the recombinamer-solvent interactions, of key relevance for the electrospinning process. Electrospinning of proteins often leads to protein denaturation due to the choice of the electrospinning solvents. Figure 2 shows the aggregation temperature profile of HRGD6 (A) and REDVx10 (B) polypeptides in TFE. The stimuli-responsive nature of both the polymers in TFE was studied using DLS measurements. The aggregate size is reported as a function of temperature.

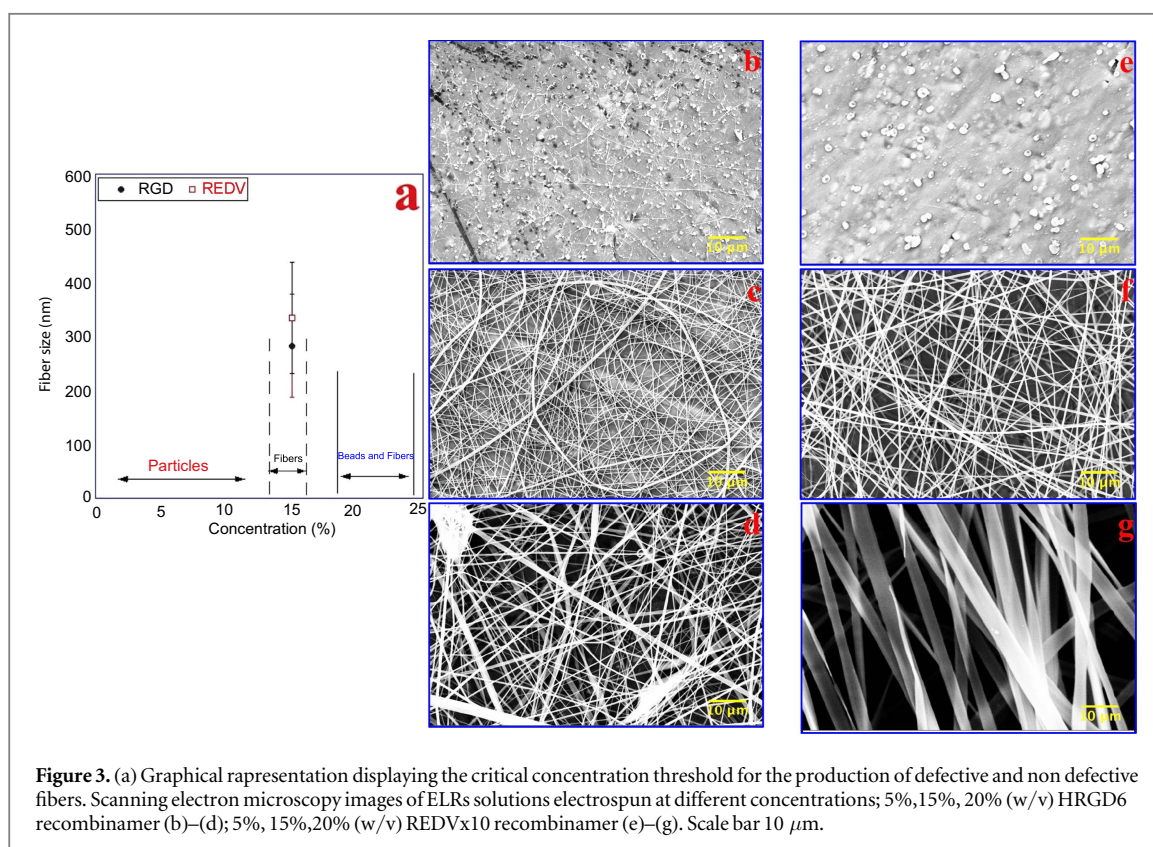
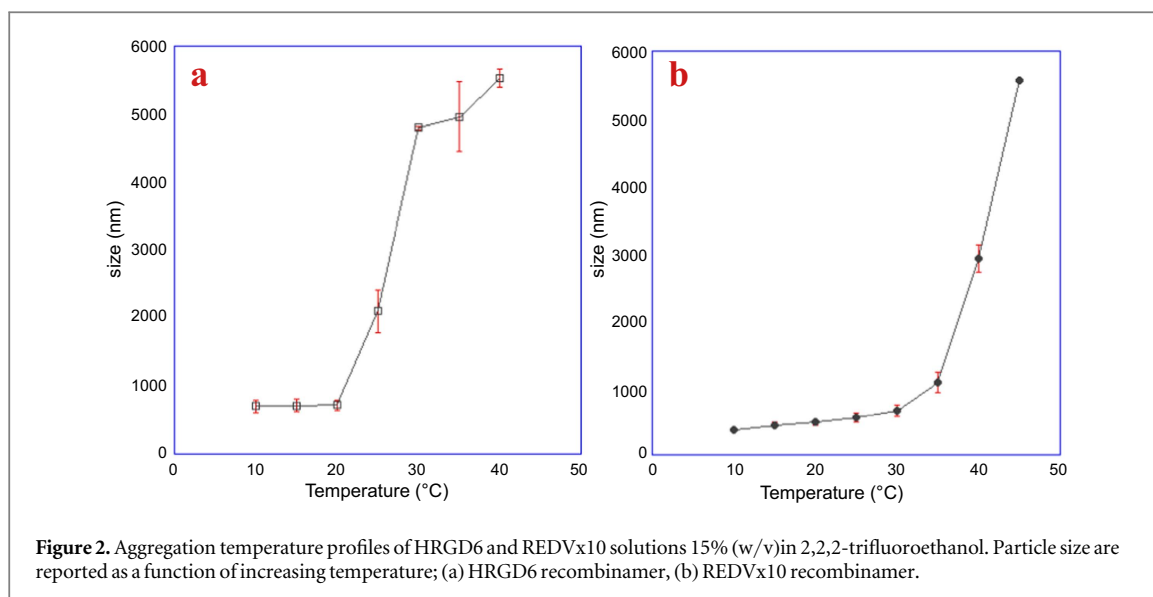
The most widely used solvents are fluoroalcohols such as 2,2,2-trifluoroethanol and 1,1,1,3,3,3-hexafluoroisopropanol, which are highly volatile (Ting *et al* 2010). Unfortunately, this fluoroalcohols denature proteins and allow the lowering of the denaturation temperature (Hong *et al* 1999). However, this fact is not particularly relevant for the used ELR as they lack any relevant tertiary structure related to their bioactivity. Collagen nanofibers fabricated using phosphate buffer saline as a solvent for the electrospinning process show only few differences from the fibers obtained using HFP (Bin *et al* 2009). Interactions between TFE and polypeptides lead to the complete dissolution of both the hydrophobic and hydrophilic block of molecules at room temperature, compared to water, which hydrates the hydrophilic portion. Thus, fibers obtained from TFE have different mechanical and morphological properties. At high TFE concentrations, intermolecular hydrogen bonding is inferred involving both $-\text{OH}$ and the $\text{C}-\text{F}$ groups of the fluoroalcohol (Blandamer *et al* 1990). Recently, an indirect mechanism for the stabilization of helices has been proposed in which the alcohol preferentially stabilizes the helical state, or indeed compact states relative to the unfolded polypeptide chain by affecting their solvation shells (Walgers *et al* 1998). Experimental data on the folding of a dimeric coiled protein suggest that this solvent mediated mechanism may be the predominant one at low cosolvent concentrations (Kentsis and Sosnik 1998).

Both ELRs were easily processed into fibers whose diameter varied between 200 and 400 nm. We started by modifying ELR concentration in order to evaluate the effect of that parameter on fiber manufacturing. By changing the concentration, it is possible to obtain a large variety of structures for both HRGD6 and REDVx10 ELRs. The effects of concentration can be seen in figure 3.

Besides the concentration that affect the fabrication of fibers and their morphology, we made a thorough study by changing different process parameters in order to obtain scaffolds free of defects and beads. Different process parameters were used for the control of the electrospinning process. The value of the minimum voltage at which the fibers are being obtained free from defects varies between 13 and 20 kV, for both recombinamers. For what concern the HRGD6 ELR, the selected values of flow rate and nozzle tip-collector distance were 0.3 ml h^{-1} and 15 cm, respectively. Figure 4 shows the effects of varying the applied voltage (A)–(C) and tip-to-collector distance (E)–(G).

In order to assess the optimization of process parameters, similar experiments were made changing only the feed rate. Scanning electron microscopy images of samples obtained are depicted in figure 5.

Similar attempts were made for the REDVx10 ELR. The results obtained increasing the applied voltage from 13 to 18 kV (feed rate 0.3 ml h^{-1} , distance 15 cm) and tip-to-collector distance from 13 to 20 cm



are shown in figure 5, respectively (A), (B), (C) for the voltage and (E), (F), (G) for the distance.

Double layer ELR meshes made of REDVx10 and HRGD6 polymers were produced using the same process parameters but increasing the time of electrospinning in order to obtain thicker layers. A new type of structure was fabricated by the electrospinning of the recombinamers. The obtained structure is formed by two layers; the innermost layer is formed by the REDVx10 polymer, which was firstly electrospun in order to promote the adhesion of endothelial cells precursors that bind through the $\alpha_4\beta_1$ integrin; the

outermost layer was obtained by the electrospinning of the HRGD6 polypeptide, which promotes adhesion to endothelial cells of the inner layer of the vessel, the intima layer. Thus, these types of structures are particularly suitable for the regeneration of the vascular tissue, due to the presence of these recognition sequences within the recombinamer. Figures 7(A) and (B) show scanning electron microscopy image of the double layer structure obtained. Using a 4 mm rotational mandrel collector, we synthesized a new double-layered vascular graft using elastin REDVx10 and HRGD6 polymers (figures 7(C) and (D)).

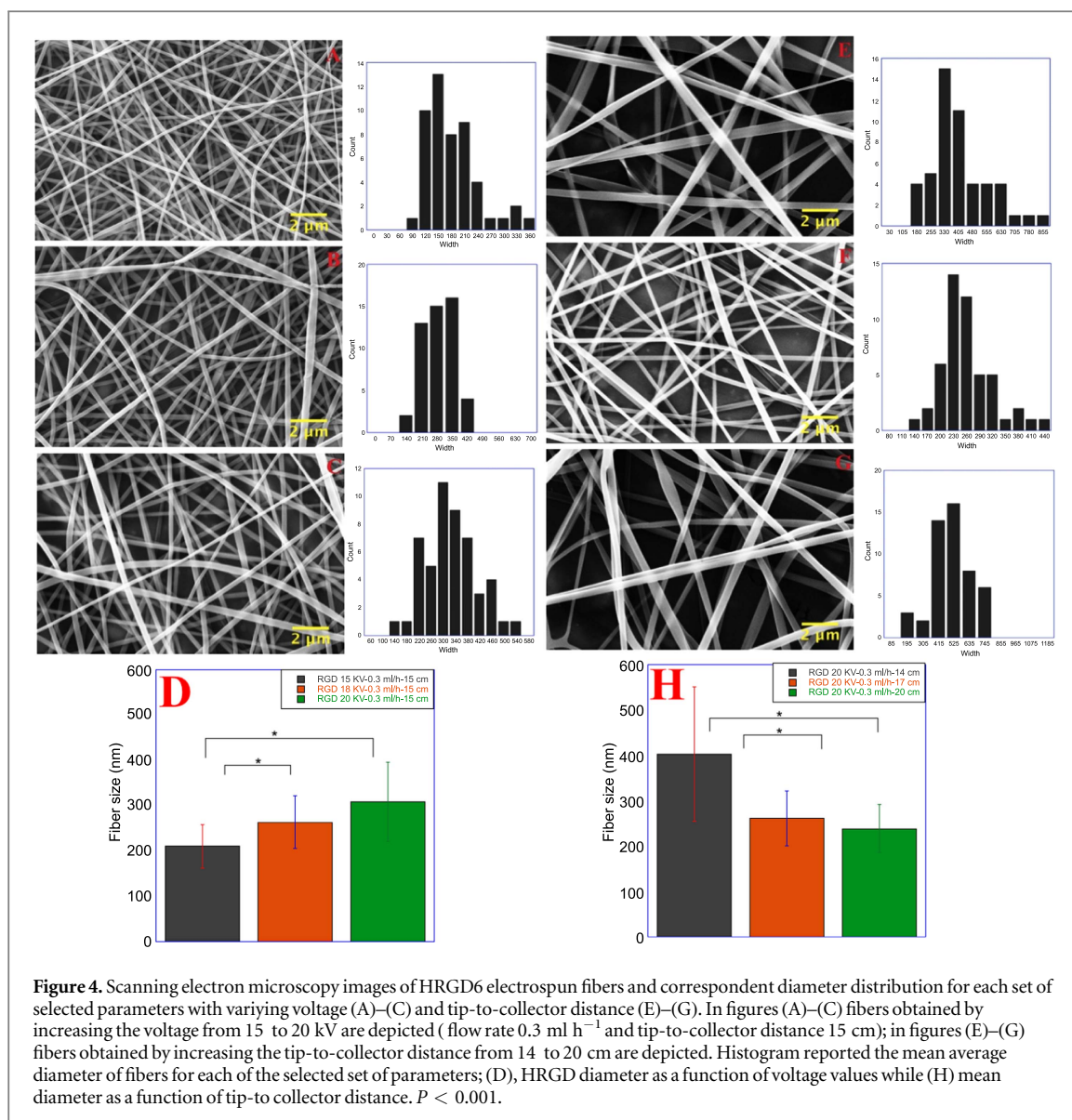


Figure 4. Scanning electron microscopy images of HRGD6 electrospun fibers and correspondent diameter distribution for each set of selected parameters with varying voltage (A)–(C) and tip-to-collector distance (E)–(G). In figures (A)–(C) fibers obtained by increasing the voltage from 15 to 20 kV are depicted (flow rate 0.3 ml h⁻¹ and tip-to-collector distance 15 cm); in figures (E)–(G) fibers obtained by increasing the tip-to-collector distance from 14 to 20 cm are depicted. Histogram reported the mean average diameter of fibers for each of the selected set of parameters; (D), HRGD diameter as a function of voltage values while (H) mean diameter as a function of tip-to collector distance. *P* < 0.001.

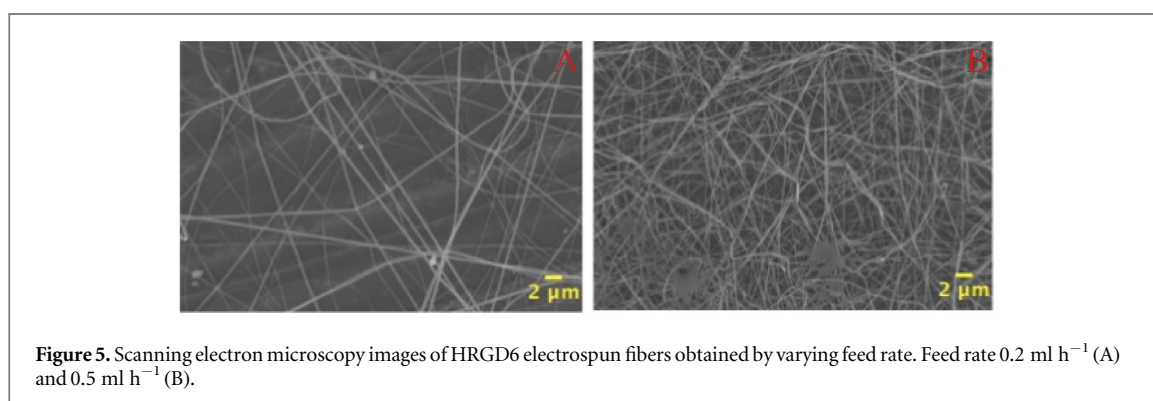


Figure 5. Scanning electron microscopy images of HRGD6 electrospun fibers obtained by varying feed rate. Feed rate 0.2 ml h⁻¹ (A) and 0.5 ml h⁻¹ (B).

All the uncrosslinked electrospun mats are highly unstable in water, leading to complete disintegration when placed in contact with an aqueous solution. In order to prevent such a fast deconstruction rate of the scaffolds, it is possible to use numerous crosslinking agents, which favor the formation of stable bonds between the polymer chains, increasing the stability of

the fibrous matrix. In this work, the double-layered ELR scaffolds made of REDVx10 and HRGD6 were chosen as a sample model to study the different behavior of endothelial cells in uncrosslinked and crosslinked genipin scaffolds. Scanning electron microscopy images reported in figure 8 show the texture of the ELR scaffold crosslinked with 0.1%

genipin/acetone solutions for 48 h. Scanning Electron microscopy images of crosslinked genipin/acetone scaffolds at 37 °C in PBS are shown in figure 8(A). Figures 8(C)–(E) show the degradation of ELRs fibrous mats in PBS for 1, 3 and 6 days. Frequency distribution of diameters for the crosslinked fibers is depicted in figure 8(F).

First adhesion and viability of HUVECs on uncrosslinked and crosslinked ELR fiber mats was measured *in vitro*, seeding cells on the HRGD6 side of the scaffolds. Preliminary contact study of HUVECs on top of double layer ELR uncrosslinked mats were done for 1, 4 and 7 days. Results are shown in figure 9.

The same experiment, previously described, was performed with genipin-crosslinked ELR scaffolds. Crosslinked scaffolds were biologically tested with HUVECs in order to evaluate the adhesion and proliferation rate. Figure 10 reported the adhesion and proliferation of HUVECs on top of double-layered ELR crosslinked scaffolds versus gelatin coated controls.

To test the viability and cytocompatibility of cells on crosslinked genipin/acetone scaffolds, we made an MTT assay. Results are reported in figure 10 as vitality of HUVEC cells as a function of seeding time.

Discussion

ELRs exhibit in TFE self-assembling properties; in particular, TFE is capable to promote hydrophobic interactions between polymer chains, which experiment a transition from the random coil to type II- β structures, forming aggregates of increasing size with increasing temperature (Reiersen and Rees 2000). Thus, the selection of 2,2,2-trifluoroethanol (TFE) was based on its chemical characteristics as its high permittivity ensures stronger polar interactions among the recombinamer chains mediated by solvent molecules; furthermore, trifluoroethanol promotes a high net charge density in solution, favoring the stretching of the fibers.

HRGD6 15% (w/v) solution in TFE aggregation profile is shown in figure 2(A). The increase in β -structures on increasing the concentration of TFE follows a sigmoidal trend. This trend is attributed to the balance present between two different structures, random coil and β -turn (Buck 1998). At low temperatures with concentrations of 100% of TFE the balance is shifted towards the random coil even if the effect of the high concentration of the solvent is evident, as it favors the formation of aggregates. Halogenated alcohols have the ability to form clusters that promote hydrophobic interactions between the side chains of the amino acids. In the case of TFE, those clusters are formed at concentrations as low as 20% (Reiersen and Rees 2000). The curve starts from 10 °C and indicates an aggregation temperature around 32 °C. At this particular temperature, the aggregate size increases

from 720 to 4900 nm. This effect is due to the stabilization of II β -turn induced by TFE. On increasing the temperature, the balance between random coil- β -turn shifts towards this latter structure. So, even at low temperatures, the effect of solvent in forming bigger aggregate sizes is stronger due to the formation of TFE clusters that can interact with hydrophobic amino acids (Reiersen and Rees 2000).

Despite ELR in water, where the transition from random coil to β -turn reaches a plateau on increasing the temperature, in this case there is a further increase in size of aggregate clusters, from 4800 to 5500 nm, between 30 °C and 40 °C. This phenomenon is due to further structural changes that affect the transition.

Even in the case of REDVx10 ELR (figure 2(B)), aggregate size measurements show an increase in particle dimension on increasing the temperature. At 40 °C there is no evident sign of transition.

The REDVx10 sequence is full of non-polar amino acids such as Valine and Proline that are known to act as chain breakers (Peizhi and Baldwin 1997). Thus, in the case of REDVx10 sequence, there is an increasing formation of β -turn on increasing the temperature due to the folding of the chain on itself and the subsequent action of the solvent that diminishes the hydrophobic interactions between non-polar residues distant in the chain (Buck 1998). Moreover, the effect of solvent is evident by the induction of cluster formation at lower temperatures.

For the fabrication of nanofibrous ELR scaffolds, we started from different polymer concentrations in order to optimize process parameters. As can be seen from the figure 3, at 5% (w/v) beads and particles are present within the samples. In this case, we can assume that the concentration of the solution is below the entanglement concentration and -thus- the semi-dilute disentanglement regime is established. Polymer entanglements are not favored and the formation of particles instead of fibers is visible for both the polymers. Increasing the concentration up to 15% (w/v), we can easily obtain fibers with a diameter in the order of nanometers. This can be explained by the increased viscosity of the recombinamer solutions and a higher number of chain entanglements leading to the formation of fibers randomly distributed onto the flat static collector. In this case, beadless fibers can be obtained through the modification of the process parameters.

Fibers with a ribbon-like structure can be obtained changing the concentration to 20%. In this case, the higher viscosity of the solution reflected a more difficult electrospinning process since the solution fails to be ejected from the needle. In figure 4 are shown fibers obtained by changing applied voltage and tip-to-collector distance. As for the voltage, no beads appear for any of the selected parameter. The diameter of the fibers was measured using ImageJ software; it was observed that by increasing the applied voltage, the average diameter increased from 180 ± 57.7 to 309 ± 87.7 nm ($p < 0.001$). In this case, the viscosity

of the solution leads to reaching the semi-dilute entangled regime thus favoring a larger amount of recombinamer ejected from the nozzle and the formation of fibers. Hence, a greater fiber diameter is produced when increasing the applied voltage. Furthermore, for low voltages the diameter distribution is not homogeneous; there is a high dispersion of the fiber diameters for voltage values of 15 and 18 kV. Conversely, a uniform diameter distribution was found for the 20 kV voltage; this distribution is in agreement with the increasing size of fibers for the chosen settings (figure 4).

The effect of tip-to-collector distance was also studied, as it increased from 14 to 20 cm (figure 4, right box). The applied voltage was kept to 20 kV and the flow rate to 0.3 ml h^{-1} ($p < 0.001$). In this case, the fiber diameter decreased significantly from 402 ± 147 to $238 \pm 53 \text{ nm}$, but the presence of some defects was more consistent. Furthermore, flattened fibers seem to be the predominant specimen. The formation of beads seems to be more influenced by the tip-to-collector distance. In fact, with increasing only distance values, the size and amount of beads did not increase (figures 4(D)–(F)). We then systematically changed the feed rate parameter and obtained different electrospun structures. Figure 5 compares the fibrous mats obtained with the two different feed rates, with an applied voltage of 13 kV and a nozzle tip-collector distance of 15 cm. Lowering the delivery rate of the solution to 0.2 ml h^{-1} the density of the deposited fibers was too poor, due to a lesser amount of material on top of the needle (figure 5(A)). Furthermore, increasing the feed rate to 0.5 ml h^{-1} yielded a significant increase in the formation of defects such as blobs and drops, which altered the fiber morphology (figure 5(B)). Thus, a value of 0.3 ml h^{-1} was chosen. Therefore, the optimum set of process parameters for the HRGD6 ELR was found to be 20 kV- 0.3 ml h^{-1} -150 mm, which proved to ensure a very good density of fiber deposition, good morphology and diameter distribution, while preventing the formation of beads.

As for the REDV polymer, results in figures 6(A)–(C) show the effect of changing the applied voltage from 15 to 18 kV. Diameter of fibers increases; the presence of beads is evident for the voltage value of 13 kV, due to the breakage of the jet and a faster evaporation of the solvent. In this case, the faster evaporation of the solvent seems to produce a local accumulation of polymer thus favoring the presence of particles instead of fibers. By increasing the voltage, the number of beads decreases and more flattened fibers appear. There is an increase in fiber size with increasing voltage, going from an average diameter of 224 ± 50 to $443 \pm 115 \text{ nm}$ ($p < 0.001$). Results obtained by varying the tip-to-collector distance from 13 to 20 cm are reported in figures 6(D)–(F). The effect of the increasing distance resulted in a reduction in the fiber diameters. Fibers showed an average diameter ranging between 271 ± 87 and $160 \pm 37 \text{ nm}$. As for the beads,

they are still noticeable for distance values of 18 and 20 cm. At 18 cm the increased distance starts to have an effect both on the morphology of the fibers and on the density of the deposited material. In fact, as shown in figure 6 (right box), the fibers have a great number of beads, a sign that the higher distance causes the breakage of the jet and the subsequent formation of defects. Jet breakage leads to a small amount of material deposited onto the collector. This phenomenon is more pronounced for higher values of distance, as shown in figure 6. As the distance increases, the number of beads increases and the material amount deposited on top of the collector decreases correspondingly (figures 6(D)–(F)).

The same process parameters used for the fabrication of the ELRs monolayers were selected for the fabrication of a new multilayered scaffold. The obtained structure is formed by two layers; the innermost layer is formed by the REDVx10 polymer, which was firstly electrospun in order to promote the adhesion of endothelial cells precursors that bind through the $\alpha_4\beta_1$ integrin; the outermost layer was obtained by the electrospinning of the HRGD6 polypeptide, which promotes adhesion to endothelial cells of the inner layer of the vessel, the intima layer. Thus, these types of structures are particularly suitable for the regeneration of the vascular tissue, due to the presence of these recognition sequences within the recombinamer. The two types of ELR fibers appear homogenous (figures 7(A) and (B)) without any kind of defects or beads. No significant differences can be found in fiber morphology for the two ELRs. Fibers are smooth; they are deposited on the collector and intertwined. Thus, in this case, the overall size is around $192 \pm 37 \text{ nm}$. The thickness of the scaffold is around $150 \mu\text{m}$ (data not show). Moreover, using a rotating mandrel we realized a double-layered vascular graft made of REDVx10 and HRGD6 polymers. A representative picture of ELR tubular scaffold is shown in figures 7(C) and (D). Even in this case, fibers appear interconnected without defects which allows the use of the composite device for *in vitro* testing with endothelial cells.

The stability of the ELRs scaffolds was improved using genipin as crosslinking agent. Scanning electron microscopy images reported in figure 8 show the texture of the ELR scaffold crosslinked with 0.1% genipin/acetone solutions for 48 h. Fibers appear flattened but without defects. The porosity of the crosslinked scaffolds does not seem to affect the stability of the fibers. The flattened morphology of the fibers is due to the action of both genipin and acetone solution that lead a decrease in porosity. Pore size is lower because of the infiltration of solvent into the fibrous matrix. Thus, all the crosslinked fiber matrices were tested for disgregation rate in PBS for 10 days, in order to evaluate their stability.

Scanning electron microscopy images of cross-linked genipin/acetone scaffolds at 37°C in PBS are

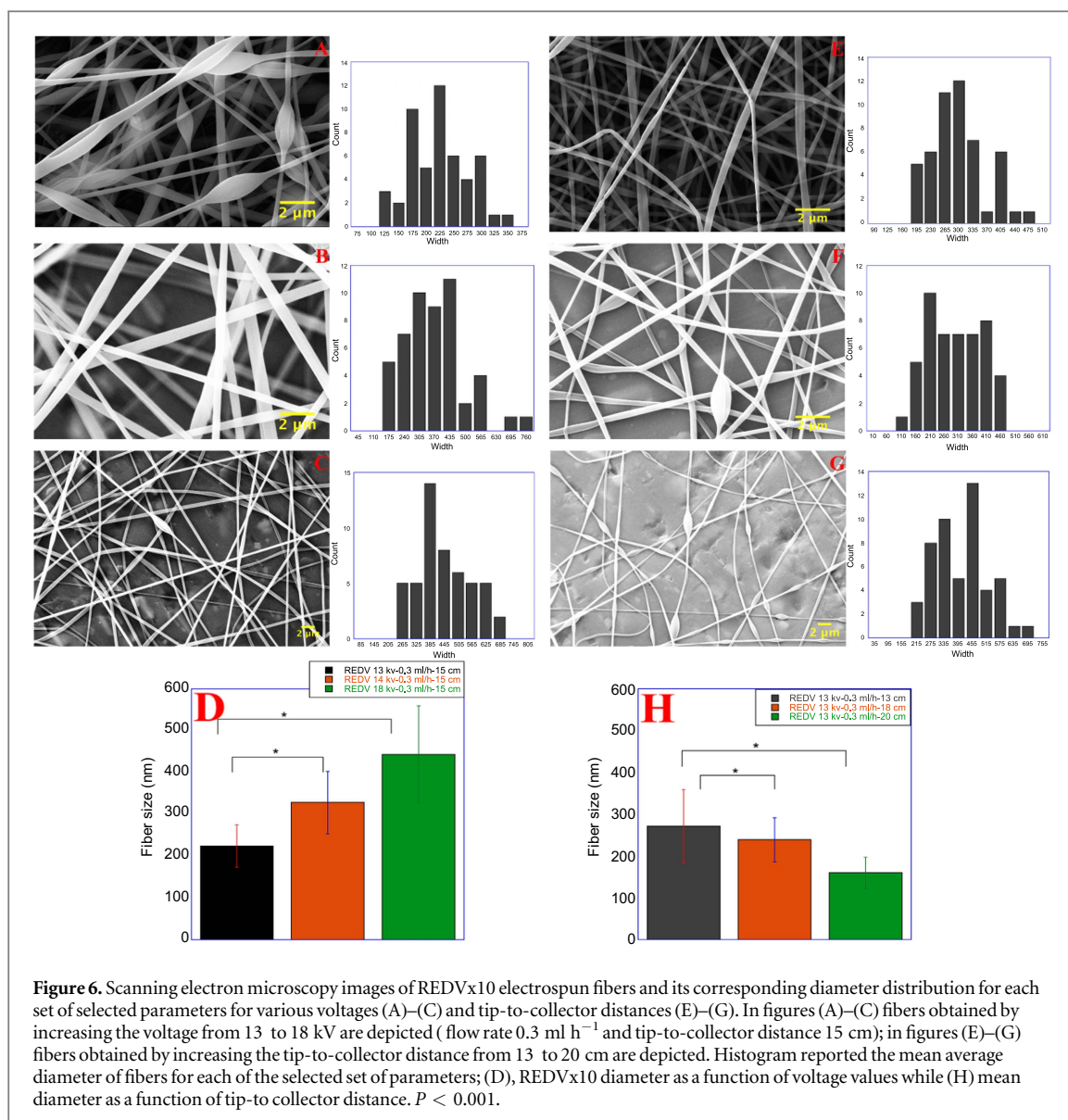


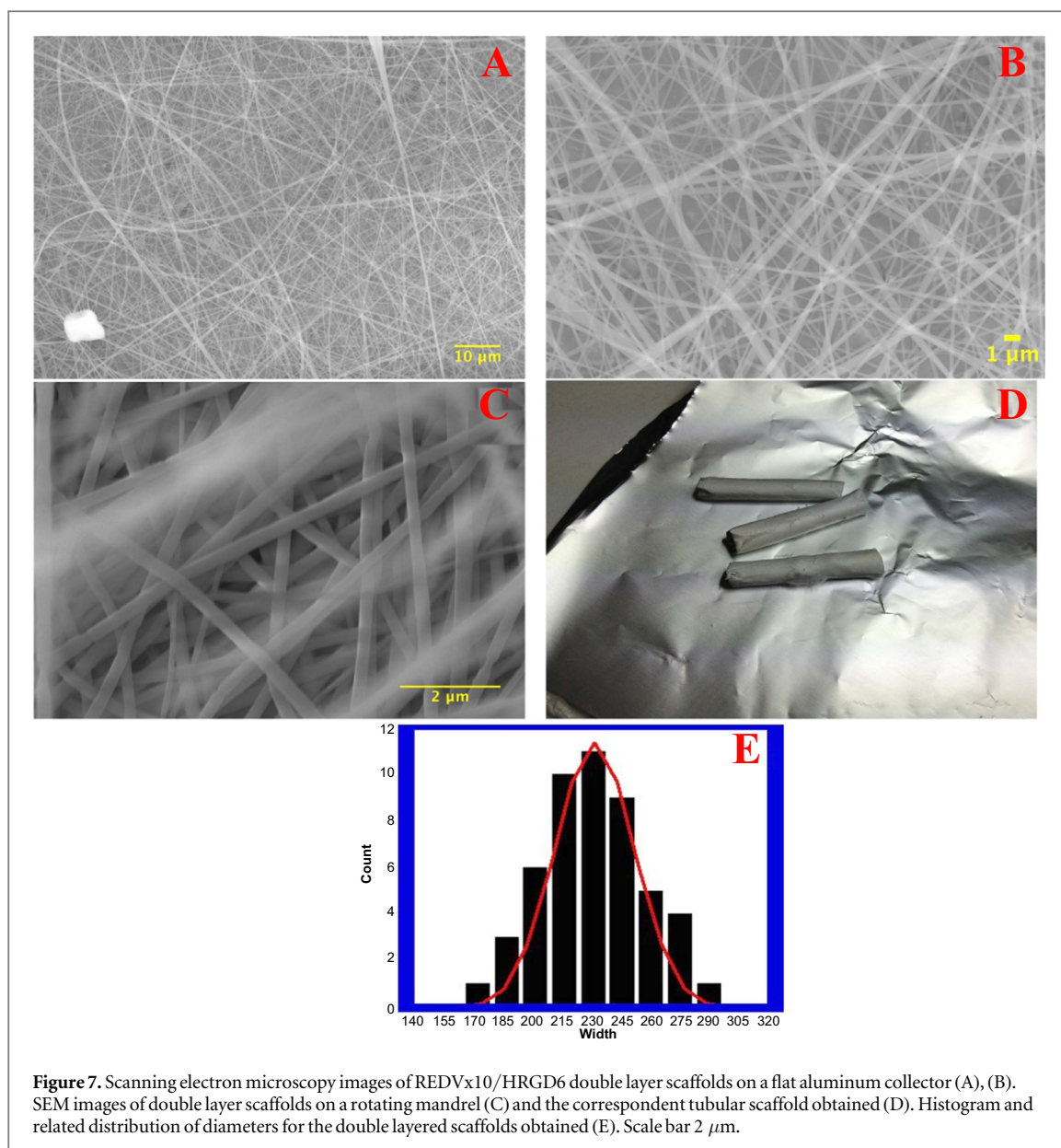
Figure 6. Scanning electron microscopy images of REDVx10 electrospun fibers and its corresponding diameter distribution for each set of selected parameters for various voltages (A)–(C) and tip-to-collector distances (E)–(G). In figures (A)–(C) fibers obtained by increasing the voltage from 13 to 18 kV are depicted (flow rate 0.3 ml h⁻¹ and tip-to-collector distance 15 cm); in figures (E)–(G) fibers obtained by increasing the tip-to-collector distance from 13 to 20 cm are depicted. Histogram reported the mean average diameter of fibers for each of the selected set of parameters; (D), REDVx10 diameter as a function of voltage values while (H) mean diameter as a function of tip-to collector distance. $P < 0.001$.

show in figures 8(A) and (B). At 24 h, fibers appear smooth and with good porosity; no defects or beads appear within the sample. Conversely, those fibers kept 3 days at 37 °C in PBS begin to take a flat shape (figure 8(C)) due to the infiltration of PBS within the matrix, which causes the reduction in porosity and the change in fiber morphology. The porosity decreases linearly with the exposure of the matrix to the aqueous environment. After 6 days, fibers are completely flat (figure 8(D)). The pores are almost gone and replaced by the flattened material. *In vitro* experiments were done in order to characterize adhesion of endothelial cells on top of crosslinked double-layered scaffolds, on HRGD6 side.

Differences in cell behavior are influenced by both topographical and biocompatible characteristics. In particular, in order to promote the interaction between biomaterial and cells, recognition sequences have to be present within the material. Recognition sequences within the polymer are able to affect cell behavior.

The ELRs used in this work were bioactivated through the insertion of RGD and REDV sequences. In particular, RGD is a common sequence involved in cellular attachment and recognition, via integrin binding. The REDV sequence is the CS5 Fibronectin tetrapeptide, which is specifically recognized by the $\alpha_4\beta_1$ integrin present in the circulating endothelial precursors cells (Rodriguez Cabello *et al* 2012). A rapid recognition and interaction of endothelial cells is mediated by the RGD sequence.

Adhesion and viability of HUVECs on uncrosslinked and crosslinked ELR fiber mats was measured *in vitro*, seeding cells on the HRGD6 side of the scaffolds. It is important to remark that uncrosslinked ELR scaffolds destructure and rapidly change their texture from a fibrous mat to a homogeneous gel-like structure. However, it is worth testing possible adhesion and proliferation of endothelial cells on the destructured homogeneous remnants of the uncrosslinked ELR bilayer electrospun scaffolds. Preliminary contact study of HUVECs on top of double layer ELR



uncrosslinked mats were done for 1, 4 and 7 days. Results are shown in figure 9. Incubation of HUVECs on top of sterilized fiber mats show no cytotoxicity, regardless of the time. At 24 h there is a high proliferation rate of cells (figures 9(D) and (E)). From optical microscope images, extensive disgregation of scaffolds is also evident (figure 9(D)). Uncrosslinked ELR scaffolds undergo a peculiar phase transition, which seems to affect cell behavior. Cells seeded onto the scaffold surface trigger the modification of the substrate texture, bringing it from a fibrous matrix to a homogeneous gel-like structure. This gel-like structure is further disgregated within the first 4 days (figures 9(F) and (G)). After seven days, disgregation of the ELR scaffold is complete, as shown in figures 9(H) and (I). Cells are totally adherent to the bottom of the plates. So, in the case of uncrosslinked ELR scaffolds, proper culture of endothelial cell cannot be carried out for periods longer than 24 h.

These results are in agreement with the *in vitro* assay where the number of adherent cells is reported as a function of seeding time (figures 9(L) and (M)). In this experiment, cells were maintained in culture for 24 h. They were seeded on top of the REDVx10/HRGD6 scaffolds on the HRGD6 side of the scaffolds and soon after began to adhere. The adhesion starts quickly and cells slightly began to proliferate at 8 h. At 24 h the adhesion is complete; endothelial cells start to increase their proliferation rate, going from 1×10^4 to 3×10^4 cells/scaffold (figure 9(M)). This higher proliferation rate with respect to the control (figure 9(L)) is probably due to the recognition sequences present within the scaffold matrix, in particular the HRGD6 that is able to promote the adhesion of cells.

The same experiment, previously described, was performed with genipin-crosslinked ELR scaffolds. Crosslinked scaffolds were biologically tested with HUVECs in order to evaluate the adhesion and

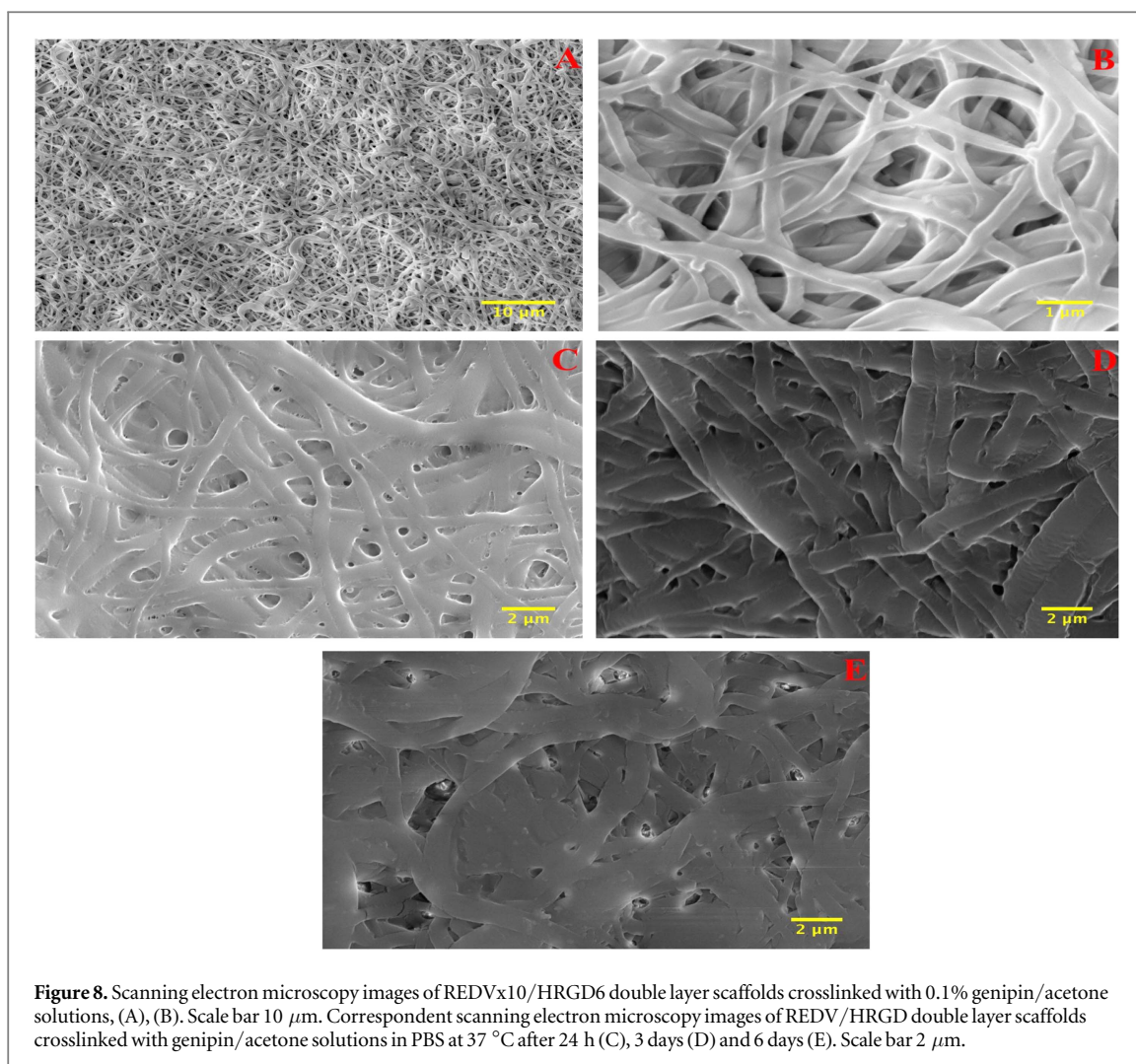


Figure 8. Scanning electron microscopy images of REDVx10/HRGD6 double layer scaffolds crosslinked with 0.1% genipin/acetone solutions, (A), (B). Scale bar 10 μm . Correspondent scanning electron microscopy images of REDV/HRGD double layer scaffolds crosslinked with genipin/acetone solutions in PBS at 37 $^{\circ}\text{C}$ after 24 h (C), 3 days (D) and 6 days (E). Scale bar 2 μm .

proliferation rate. Figure 10 reported the adhesion and proliferation of HUVECs on top of double-layered ELR crosslinked scaffolds versus gelatin coated controls. At 4 h, the adhesion of cells is almost similar for the crosslinked and uncrosslinked scaffold (figures 10(A) and (D)). A higher rate of adhesion for the ELR crosslinked samples is evident at 8 h where is evident an initial proliferation of cells that settles to 2.5×10^4 (figure 10(E)). This is due to a higher stability of the crosslinked substrate that maintains its fibrous texture contrarily to the uncrosslinked one. As for the proliferation rate of cells, the increasing number is related to the higher porosity and stability of the crosslinked scaffold (figure 10(I)). Genipin crosslinked scaffolds allow the adhesion and infiltration of cells, thus favoring their proliferation that increases up to 3.8×10^4 , at 24 h. Moreover, cells on top of the cross-linked scaffolds appear more spread after 24 h (figure 10(F)). The flat morphology of the fibers within the scaffold does not appear to negatively affect the adhesion of cells, as shown in the confocal images (figures 10(D)–(F)). In the case of crosslinked scaffolds there is an increasing cell adhesion that is associated

with an increased sprouting of cells (figure 10(F)). This seems to be due to a better stability of the scaffold and to an increase in its porosity. Porosity has a positive effect on cell behavior as it causes increased cell infiltration within the fibrous matrix. The cellular behavior can be summarized in two distinct phases: during the initial phase, the high stability of the scaffold and the presence of cell-adhesion sequences (REDV and RGD) within the structure favor the adhesion of HUVECs to the surface. Later, thanks to the high porosity of the scaffold, the cells begin to proliferate and sprout. This step is much more evident in the case of the genipin-crosslinked scaffolds, at 24 h as reported in figures 10(D)–(F).

In figure 11(A) MTT assay histogram is reported. As it can be seen, number of live cells increases linearly with the seeding time meaning that scaffold matrices and the presence of the RGD recognition sequence improved the stability of scaffold and the viability of cells *in vitro*. Moreover, these data are in accordance with our preliminary results of HUVEC adhesion on top of crosslinked scaffolds.

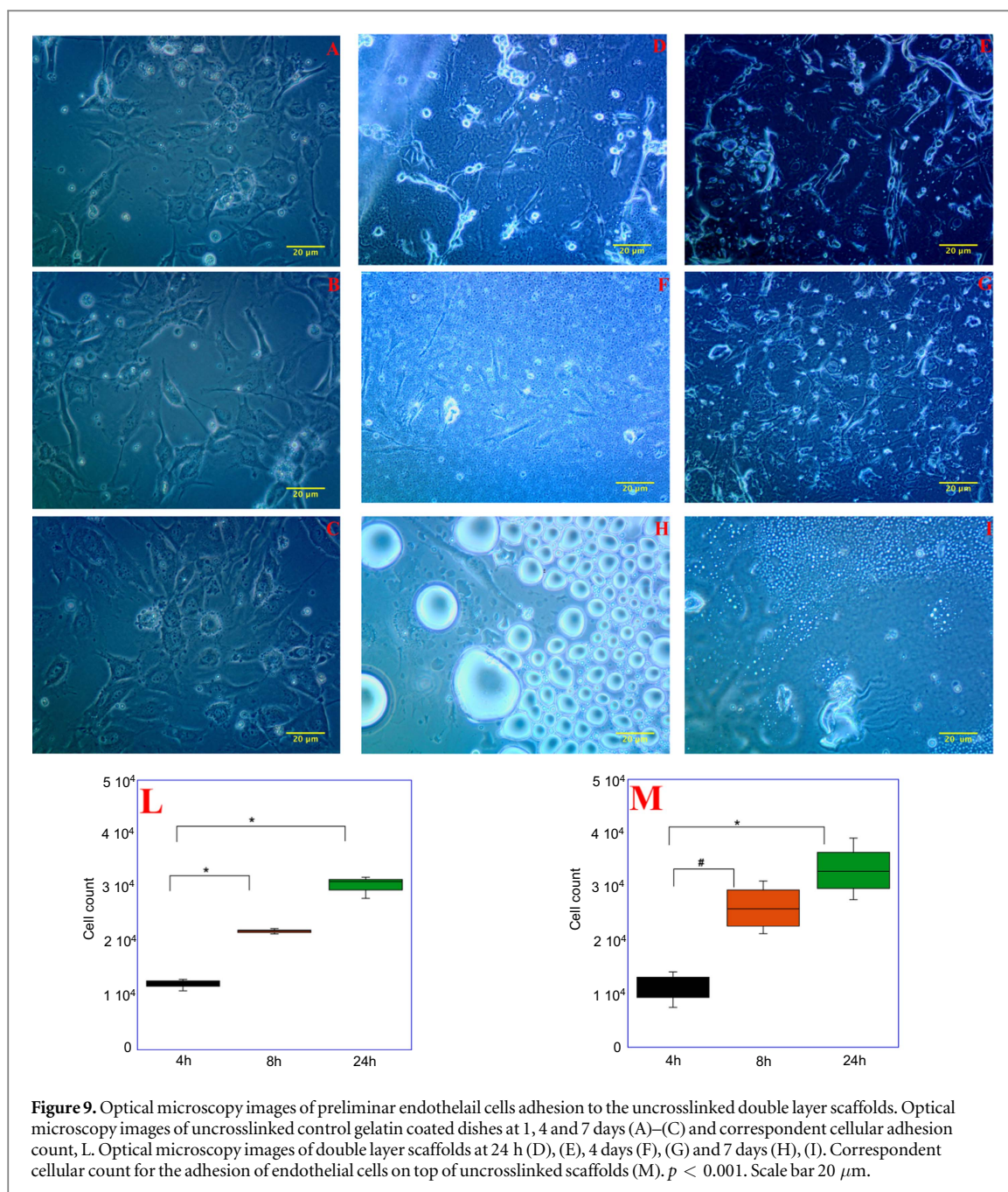


Figure 9. Optical microscopy images of preliminar endothelial cells adhesion to the uncrosslinked double layer scaffolds. Optical microscopy images of uncrosslinked control gelatin coated dishes at 1, 4 and 7 days (A)–(C) and correspondent cellular adhesion count, L. Optical microscopy images of double layer scaffolds at 24 h (D), (E), 4 days (F), (G) and 7 days (H), (I). Correspondent cellular count for the adhesion of endothelial cells on top of uncrosslinked scaffolds (M). $p < 0.001$. Scale bar 20 μm .

Conclusions

In this work, we describe the fabrication of a new bioresorbable scaffold for tissue regeneration in cardiovascular diseases. We made a thorough characterization of the ELR solutions in TFE. Fibers without beads and defects were obtained by varying recombinant concentrations and process parameters. The obtained scaffolds were used for the *in vitro* assays to determine adhesion and proliferation of HUVECs. A relatively fast de-structuring of the scaffolds can be observed when the electrospun ELR fiber were not crosslinked. Such disgregation could be avoided by a further crosslinking of the ELRs forming the fibers by using genipin as a crosslinking agent. The scaffolds so obtained were tested *in vitro* with HUVECs. The

crosslinking procedure prevents the de-structuring and disgregation processes and allows the complete adhesion, proliferation and sprouting of cells on the top of the crosslinked scaffolds. The genipin crosslink induces a higher stability of the fibrous matrix, as reflected by the increasing number of cells that can adhere to the scaffold surface. Moreover, cytocompatibility assay proved the viability of HUVEC cells maintained in culture for longer periods.

A tubular ELR composite device, made of a double layer of REDV/HRGD6, was fabricated by using a rotating mandrel collector. This tubular scaffold shows a good fiber morphology, absence of any defects and a uniform distribution of diameters. Tubular scaffolds made of ELRs could be useful for the regeneration of the arterial intima layer of vessels.

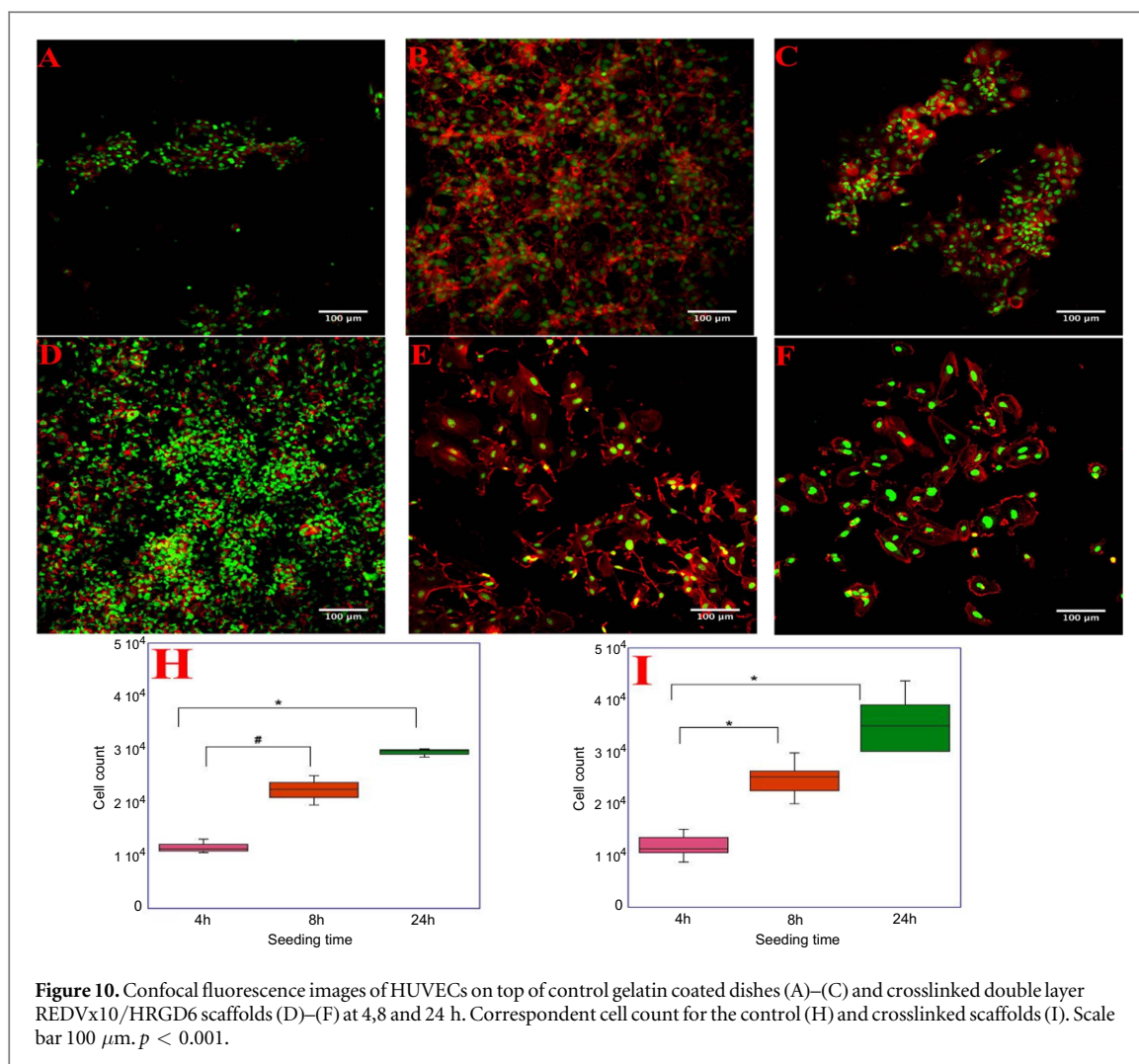


Figure 10. Confocal fluorescence images of HUVECs on top of control gelatin coated dishes (A)–(C) and crosslinked double layer REDVx10/HRGD6 scaffolds (D)–(F) at 4, 8 and 24 h. Correspondent cell count for the control (H) and crosslinked scaffolds (I). Scale bar 100 μm. $p < 0.001$.

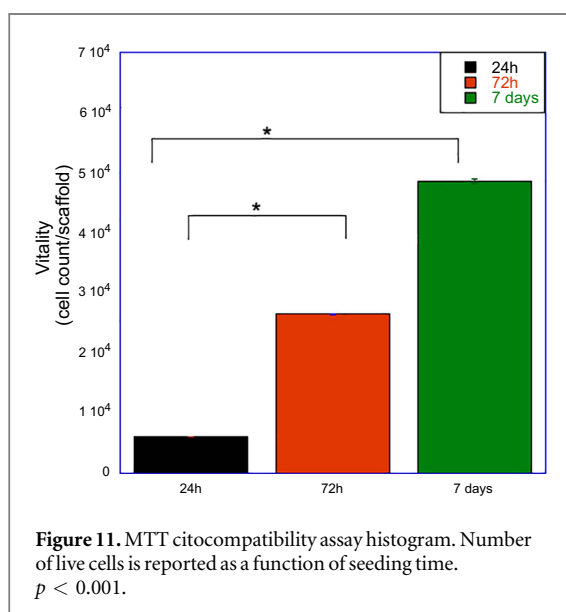


Figure 11. MTT citocompatibility assay histogram. Number of live cells is reported as a function of seeding time. $p < 0.001$.

Acknowledgments

This research was supported by funds provided through ‘THE GRAIL’ (Tissue in Host Engineering

Guided Regeneration of Arterial Intima Layer) project. The project is funded by the European Union’s ‘Seventh Framework’ Programme for research, technological development and demonstration under Grant Agreement n° HEALTH.2011.1.4-2-278557. Authors thank Dr Vincenzo Guarino, Institute of Polymers, Composites and Biomaterials, National Research Council of Italy for introducing authors in the use of electrospinning machine in the case of polymer solutions.

References

- Bin D, Oliver A, Meghan E S and Gary E W 2009 Electrospinning of collagen nanofiber scaffolds from benign solvents *Macromol. Rapid Commun.* **30** 539–42
- Blandamer M J, Burgess J, Cooney A, Cowles H J, Horn I M, Martin K J and Morcom K W 1990 Excess molar gibbs energies of mixing of water and 1,1,1,3,3,3-hexafluoropropan-2-ol mixtures at 298.15 K comparison of thermodynamic properties and inverse kirkwood-buff integral functions for binary aqueous mixtures formed by ethanol, propan-2-ol, 2,2,2-trifluoroethanol and 1,1,1,3,3,3-hexafluoropropan-2-ol *J. Chem. Soc. Faraday Trans.* **86** 2209–22
- Garcia-Arevalo C, Pierna M, Girotti A, Arias F J and Rodriguez-Cabello J C 2012 A comparative study of cell

- behavior on different energetic and bioactive polymeric surfaces made from elastin-like recombinamers *Soft Matter* **8** 3239–49
- Hong D P, Hoshino M, Kuboi R and Goto Y 1999 Clustering of fluorine-substituted alcohols as a factor responsible for their marked effects on protein and peptides *J. Am. Chem. Soc.* **121** 8427–33
- Kentsis A and Sosnik T R 1998 Trifluoroethanol promotes helix formation by destabilizing backbone exposure: desolvation rather than native hydrogen bonding defines the kinetic pathway of dimeric coiled coil folding *Biochemistry* **37** 14613–22
- MacHale M K, Setton L A and Chilkoti A 2006 Synthesis and *in vitro* evaluation of enzymatically cross-linked elastin polypeptides gel for cartilaginous tissue repair *Tissue Eng.* **11** 1768–79
- Martin L, Castro E, Ribeiro A, Alonso M and Rodriguez-Cabello J C 2012 Temperature-triggered self-assembly of elastin-like block co-recombinamers: the controlled formation of micelles and vesicles in aqueous medium *Biomacromolecules* **13** 293–8
- Panzavolta S, Michela Gioffré, Focarete M L, Gualandi C, Foroni L and Bigi A 2011 Electrospun gelatin nanofibers: optimization of genipin cross-linking to preserve fiber morphology after exposure to water *Acta Biomaterialia* **7** 1702–9
- Qijin L, Ganesan K, Simionescu D T and Vyavahare N R 2004 Novel porous aortic elastin and collagen scaffolds for tissue engineering *Biomaterials* **25** 5227–37
- Ribeiro A, Arias F J, Reguera J, Alonso M and Rodriguez-Cabello J C 2009 Influence of the molecular architecture of the inverse temperature transition of elastin-like-polymers *Biophys. J.* **97** 312–20
- Rodriguez Cabello C J, Girotti A, Ribeiro A and Arias F J 2012 Synthesis of genetically engineered protein polymers (recombinamers) as an example of advanced self-assembled smart materials *Nanotechnology in Regenerative Medicine: Methods and Protocols (Methods in Molecular Biology vol 811)*
- Rodriguez Cabello C J, Martin L, Alonso M, Arias F J and Testera A M 2009 Recombinamers as advanced materials for the post-oil age *Polymer* **50** 5159–69
- Rodriguez Cabello C J, Martin L, Girotti A, Garcia-Arevalo C, Javier Arias F and Alonso M 2011 Emerging applications of multifunctional elastin-like recombinamers *Nanomedicine* **6** 111–22
- Rosamond W et al (American Heart Association Statistics Committee and Stroke Statistics Subcommittee) 2007 Heart disease and stroke statistics-2007 update: a report from the American Heart Association Statistics Committee and Stroke Statistics Subcommittee *Circulation* **115** e69–171
- Shinoka T et al 1998 Creation of viable pulmonary artery autografts through tissue engineering *J. Thorac. Cardiovasc. Surg.* **115** 536–46
- Sill T J and von Recum H A 2008 Electrospinning: Applications in drug delivery and tissue engineering *Biomaterials* **29** 1989–2006
- Smith L R et al 1991 Determinants of early versus late cardiac death in patients undergoing coronary artery bypass graft surgery *Circulation* **84** (5 Suppl) 245–53
- Suryapranata H, de Feyter P J and Serruys P W 1988 Coronary angioplasty in patients with unstable angina pectoris: is there a role for thrombolysis? *J. Am. Coll. Cardiol.* **12** A69–77
- Teo W E, Inai R and Ramakrishna S 2011 Technological advances in electrospinning of nanofibers *Sci. Technol. Adv. Mater.* **12** 013002
- Ting L, Teng W K, Chan B P and Sing yan C 2010 Photochemical crosslinked electrospun collagen nanofibers: synthesis, characterization and neural stem cell interactions *J. Biomed. Mater. Res.* **95A** 276–82
- Urry D W 1992 Free-energy transduction in polypeptides and proteins based on inverse temperature transitions *Prog. Biophys. Mol. Biol.* **57** 23–57
- Walgers R, Lee T C and Cammers-Goodwin A 1998 An indirect chaotropic mechanism for the stabilization of helix conformation of peptides in aqueous trifluoroethanol and hexafluoro-2-propanol *J. Am. Chem. Soc.* **120** 5073–9
- Watanabe M et al 2001 Tissue-engineered vascular autograft: inferior vena cava replacement in a dog model *Tissue Eng.* **7** 429–39
- Wise S G, Byrom M J, Waterhouse A, Bannon P G, Ng M K C and Weiss A S 2011 A multilayered synthetic human elastin/polycaprolactone hybrid vascular graft with tailored mechanical properties *Acta Biomater.* **7** 295–303